

Dynamic scaling and stochastic fractal in nucleation and growth processes

Amit Lahiri[†], Md. Kamrul Hassan[†], Bernd Blasius[§] and Jürgen Kurths[‡]

[†] *University of Dhaka, Department of Physics, Theoretical Physics Division, Dhaka 1000, Bangladesh*

[§] *Institute for Chemistry and Biology of the Marine Environment (ICBM)*

Carl-von-Ossietzky University Oldenburg PF 2503, 26131 Oldenburg, Germany

[‡] *Potsdam Institute for Climate Impact Research (PIK), Postfach 601203, 14412 Potsdam, Germany*

A class of nucleation and growth models of a stable phase (S-phase) is investigated for various different growth velocities. It is shown that for growth velocities $v \sim s(t)/t$ and $v \sim x/\tau(x)$, where $s(t)$ and τ are the mean domain size of the metastable phase (M-phase) and the mean nucleation time respectively, the M-phase decays following a power law. Furthermore, snapshots at different time t are taken to collect data for the distribution function $c(x, t)$ of the domain size x of M-phase are found to obey dynamic scaling. Using the idea of data-collapse we show that each snapshot is a self-similar fractal. However, for $v = \text{const.}$ like in the classical Kolmogorov-Johnson-Mehl-Avrami (KJMA) model and for $v \sim 1/t$ the decay of the M-phase are exponential and they are not accompanied by dynamic scaling. We find a perfect agreement between numerical simulation and analytical results.

PACS numbers: 68.55.Ac, 64.70.Kb, 61.50.Ks

A class of nucleation and growth process is studied analytically by solving an integro-partial differential equation and verified numerically by Monte Carlo simulation. The growth velocity is defined as the ratio of the distance traveled s by the new phase and the magnitude of time t is needed to travel that distance. We first choose constant growth velocity by assuming both s and t equal to constant and reproduce the results of the much studied classical Kolmogorov-Johnson-Mehl-Avrami (KJMA) model. Choosing one of them a constant still makes the exponential decay of the meta-stable phase like the KJMA model. However, the growth velocity is so chosen that neither s nor t is constant we find that the meta-stable phase decays following a power-law. Such power-law is also accompanied by the emergence of fractal. The self-similar property of fractal is verified by showing that the system exhibits dynamic scaling revealing a self-similar symmetry along the continuous time axis. According to Noether's theorem there must exist a conserved quantity and we do find that the d_f th moment, where d_f is the fractal dimension, is always conserved.

I. INTRODUCTION

The formation of any phase is usually a process that starts first by nucleation of new phase on old phase, which is called metastable phase, followed by growth of the new phase which eventually becomes a stable phase (S-phase). This mechanism of nucleation and growth represents one of the most fundamental topics of interest in both science and technology [1]. It plays a key role in metallurgical applications as well as in many seemingly unrelated fields of research. Phase separation and coarsening [2], elec-

trodeposition of metals at electrodes via nucleation and growth [3], melting of stable glasses [4], dendritic growth [5], kinetics of crystal growth [6], the domain switching phenomena in ferroelectrics [7], the spread of ecological invaders [8] and growth of breath figures [9] are just a few examples of such systems. Besides, G. Giacomelli et al. studied an interesting case in which nucleation occurs in time not in space [10]. The nature of phase transition, which is governed by nucleation and growth of domains of S-phase, is well-known as first order phase transition. One of the characteristic features is that during the transition stable and metastable regions coexist at the same time. Much of our theoretical understanding of such phenomena is provided by the Kolmogorov-Johnson-Mehl-Avrami (KJMA) model, which has been formulated independently by Kolmogorov, Johnson and Mehl and Avrami in and around the 1940s [11]. This model still remains one of the most studied theories of nucleation and growth processes as it is often the only means of interpreting the experimental data that help gain insights into the process.

The KJMA theory is valid under the assumptions that (a) nucleation events are Poissonian in nature, (b) seeds grow with constant velocity while keeping fixed geometrical shape and orientation, and (c) the system is homogeneous in space and time. In the context of nucleation and growth phenomena, one of the central quantities of interest is the fraction of the M-phase $\Phi(t)$ that still survives at time t . According to the KJMA theory, this quantity in d dimensions follows an exponential decay known as the Kolmogorov-Avrami law

$$\Phi(t) = \exp \left[- \frac{\Omega_d}{d+1} \Gamma v_s^d t^a \right], \quad (1)$$

where, the Avrami exponent $a = d + 1$ [11], Γ describes the constant nucleation rate per unit volume and Ω_d is the constant volume factor of the d dimensional hypersphere e.g., $\Omega_d = 1, \pi, 4\pi/3$ for $d = 1, 2, 3$ respectively.

The derivation of correlation functions and their connection to the scattering cross-section [12, 13], the theory of grain-size populations [14], and the generalization of the KJMA theory to multiple stable phases [15] etc. have played a significant role in understanding the phenomena. Besides, these studies have provided a better means of interpreting the experimental data. On the other hand, there have been reports that the experimental data in some cases do not fit a straight line in the plot of $\log(-\log[\Phi(t)])$ against $\log[t]$ revealing that it violates the Kolmogorov-Avrami law [16, 17]. Recently, it has also been observed that nucleation and growth processes results in the emergence of fractal [18–22]. Obviously, constant growth velocity does not result in fractal. However, the nature of growth mechanism responsible for the emergence of fractal is not yet fully understood. This observation clearly raises some concerns and hence it requires further theoretical interest in order to find variants of the model which would be suitable under different physical situations. This is exactly the purpose of the present work.

In this article, we investigate a class of Kolmogorov-Johnson-Mehl-Avrami nucleation and growth model in one dimension for four different choices of the growth velocities. In particular, we choose (A) $v = \text{const.}$, (B) $v = \sigma/t$, (C) $v = ks(t)/t$ and (D) $v = mx/\tau(x)$ where σ , k and m are constants, $s(t)$ is the mean domain size and $\tau(x)$ is the mean nucleation time [23]. The idea to move away from the constant growth velocity is born by the observation that a growth velocity which may change in the course of time and space. Such choices may provides a more realistic description and hence will become more suitable under various natural conditions than constant growth velocity. Usually, as the time proceeds, size and shape of both phases change continuously, altering the condition that ultimately determines the growth velocity. We solve the corresponding rate equation for each choice of the growth velocity and obtain the exact solution for the domain size distribution function $c(x, t)$ of M-phase. Alongside, we also give exact algorithm for each case to solve them by numerical simulation. Using the idea of data collapse we show that the analytical results are in perfect agreement with our numerical simulations. It has been found that the M-phase decays exponentially with time for models (A) and (B) whereas in the case of models (C) and (D), it decays following a power-law. Moreover, the domain size distribution function $c(x, t)$ of models (C) and (D) is found to obey dynamic scaling $c(x, t) \sim t^{\theta z} \phi(x/t^z)$ revealing that it evolves with time in a self-similar fashion and eventually emerges as fractal. We find the kinetic exponent $z = 1$ and the mass exponent $\theta = 1 + d_f$. Their numerical values are fixed by the dimensional consistency and the conservation principle.

The rest of this article is organized as follows. Section II formulates the rate equation for nucleation and growth model in one dimension. We also attempt to solve the rate equation for generalized growth velocity. In Section III-VI, we solve the rate equation for four dif-

ferent growth velocities and discuss the corresponding scaling theory. For each choice of the growth velocity exact algorithm is given and extensive Monte Carlo simulation is performed to corroborate all the analytical results namely decay of the M-phase, fractal dimension, a conserved moment and dynamic scaling. In Section VII, we make concluding remarks and leave some open questions.

II. FORMULATION OF THE RATE EQUATION

The right choice of the growth velocity should depend on the detailed nature of the system under investigation. In the present work, we make a few simple choices so that we can handle the problem analytically. Further, we took extra care on the dimensional consistency with the terms describing the nucleation mechanism. Our aim is to learn how much effect the growth velocity alone has on the dynamics of the system. To obtain a mathematical formalism of the phenomena, we find it useful to treat nucleation and growth mechanisms separately and derive their respective governing equations. To do it, we define the distribution function $c(x, t)$ as the concentration of domain size x of M-phase at time t . First, we derive the rate equation for the nucleation mechanism. The random nucleation of seeds of S-phase can be thought of as a random sequential adsorption (RSA) of monodisperse, size-less particles on a substrate of M-phase. The distribution function $c(x, t)$ then obeys the following well known rate equation for RSA [13, 24]

$$\left. \frac{\partial c(x, t)}{\partial t} \right|_{\text{nucleation}} = -x c(x, t) + 2 \int_x^\infty c(y, t) dy. \quad (2)$$

The two terms on the right hand side of Eq. (2) represent the decrease and increase of M-phase intervals of size x due to the nucleation of point-like seeds of S-phase at locations x , and $y > x$, respectively. The factor 2 in the integral term takes into account that every nucleation event creates two new domains of M-phase either of which can be of size x .

To derive an expression for the growth mechanism, we consider that once a seed of S-phase has nucleated at some point on M-phase, it keeps growing with some velocity $v(x, t)$. Here we assume a simplified generalized case where the growth velocity may depend on the size x of the M-phase and the time t . In general, the growth velocity may also depend on the size of the S-phase segment, but that goes beyond the scope of the present work. To derive the growth equations, note that the growth of the S-phase occurs at the expense of the decay of the M-phase. That is, the size of the M-phase on either side of the growing seeds are shrinking with the same velocity v with which seeds of the S-phase are growing. The growth term can be deduced by taking into account all the possible ways in which the distribution function $c(x, t)$ remains in the domain size range $[x, x + dx]$ after a span of

infinitesimal time dt

$$c(x, t + dt) = [1 - 2v(x, t)dt/dx]c(x, t) + [2v(x + dx, t)dt/dx]c(x + dx, t). \quad (3)$$

Here, $v(x, t)dt/dx$ is the fraction of concentration $c(x, t)$ that is lost in time dt due to the growth of the S-phase with velocity $v(x, t)$, and the factor 2 takes into account of the fact that M-phase segments are reduced from both sides. Thus

$$\left. \frac{\partial c(x, t)}{\partial t} \right|_{\text{growth}} = 2 \frac{\partial}{\partial x} [v(x, t)c(x, t)] \quad (4)$$

Putting the nucleation and growth terms together, the general rate equation for the random nucleation followed by space-time dependent continuous growth therefore is

$$\begin{aligned} \frac{\partial c(x, t)}{\partial t} &= -xc(x, t) + 2 \int_x^\infty c(y, t)dy \\ &+ 2 \frac{\partial}{\partial x} [v(x, t)c(x, t)]. \end{aligned} \quad (5)$$

We now attempt to solve Eq. (5) subject to the initial conditions

$$c(x, 0) = \frac{1}{L} \delta(x - L), \quad \lim_{L \rightarrow \infty} \int_0^\infty c(x, 0)dx = 0. \quad (6)$$

This ensures that there is no seed of the S-phase at $t = 0$. Once we know $c(x, t)$, we can immediately find the fraction of the M-phase that remained un-transformed

$$\Phi(t) = \int_0^\infty xc(x, t)dx \quad (7)$$

and the number density of the domain size of the M-phase

$$N(t) = \int_0^\infty c(x, t)dx. \quad (8)$$

The fraction of the M-phase covered by the S-phase is related to $\Phi(t)$ via $\theta(t) = 1 - \Phi(t)$ that evolves with time as

$$\frac{d\theta(t)}{dt} = \int_0^\infty v(x, t)c(x, t)dx. \quad (9)$$

The quantities $\Phi(t)$ and $N(t)$ can also be used to obtain the time dependence of the average interval size $s(t) = \Phi(t)/N(t)$.

In the context of the present work, it is the choice of the growth velocity $v(x, t)$ that will define different models and accordingly we study the following four different choices: (A) $v(x, t) = v_0$, the traditional constant growth velocity (classical KJMA model), (B) $v(x, t) = \sigma/t$ where σ is a constant and bears the dimension of length, (C) $v(x, t) = s(t)/t$ where $s(t)$ is the mean interval size of the M-phase at time t and finally (D) $v(x, t) = mx/\tau(x)$ where $\tau(x)$ is the mean nucleation time and m is a dimensionless positive constant [23].

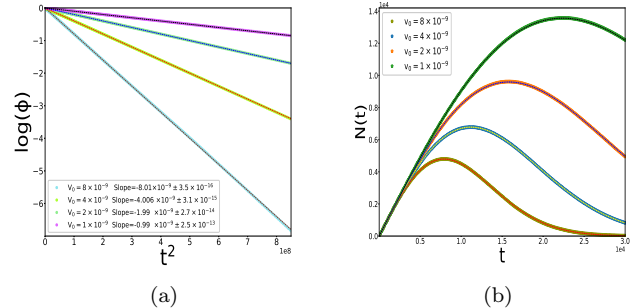


FIG. 1: (a) We plot $\log(\phi(t))$ versus t^2 for different constant growth velocities to see how the M-phase $\phi(t)$ decays with time. (b) Plots of $N(t)$ versus t is shown for different constant growth velocities.

For growth velocities $v = v(t)$ which are independent of the variable x (as in our models (A) - (C)), the general solution of Eq. (5) can be obtained by substituting the ansatz

$$c(x, t) = A(t) \exp[-xt]. \quad (10)$$

Here, the time dependent pre-factor $A(t)$ obeys the following ordinary differential equation

$$\frac{d \ln A(t)}{dt} = 2/t - 2v(t)t. \quad (11)$$

We have to solve Eq. (11) subject to the initial condition $A(0) = 0$, followed by Eq. (6). To proceed further and for clarity, we will treat for every choice of growth velocity separately and independently.

First, we note that the time dependence of $s(t)$ is independent of $A(t)$

$$s(t) = \frac{\Phi(t)}{N(t)} = \frac{A(t) \int_0^\infty x \exp[-xt] dx}{A(t) \int_0^\infty \exp[-xt] dx}. \quad (12)$$

Solving the integrals we find that in this case of $v = v(t)$ the mean interval size of M-phase shrinks as

$$s(t) = 1/t. \quad (13)$$

In choosing the growth velocity, we shall make use of this relation. Interestingly, the same expression also holds for a model without the growth term which is known as random scission model [25].

III. MODEL A

We first consider the classical KJMA model defined by the constant velocity of domain of S-phase $v(t) = v_0$. The goal is to reproduce the known results so that they help build confidence on the rate equation approach and help appreciate its simplicity. Solving the problem rest on finding the distribution function $c(x, t)$ which

means coding all the essential information regarding this model. After substitution of $v(t) = v_0$ into Eq. (11) and a straightforward integration we immediately obtain $A(t) = t^2 \exp[-v_0 t^2]$ and the solution of Eq. (5) for the classical KJMA model is given by

$$c(x, t) = t^2 \exp[-xt - v_0 t^2]. \quad (14)$$

Using this in the definition of $\Phi(t)$, we immediately find that

$$\Phi(t) = \exp[-v_0 t^2]. \quad (15)$$

It implies that the plots of $\log(\Phi(t))$ versus t^2 should give a straight line with slope equal to $-v_0$. This is indeed the case as shown in Fig. (1a). Note that $v_s = 2v_0$ where v_0 is the velocity of front of the S-phase that moves forward transforming the M-phase into S-phase within it. Thus, the velocity with which each seed grows is $v_s = 2v_0$ and substituting it into the expression for $\Phi(t)$, we can immediately recover the celebrated Kolmogorov-Avrami law in one dimension as given in Eq.(1), except the factor Γ . Note that Eq. (2) describes the random sequential nucleation of one seed at each time step and hence $\Gamma = 1$ in the context of the present rate equation approach. The rate equation approach thus clearly demonstrates its simplicity and brevity. This is however true only for one dimension. In the context of nucleation and growth phenomena, the 1d model can in fact fully capture the qualitative behavior of the key quantities of interest, namely the decay of the M-phase. The Kolmogorov-Avrami law itself is a testament to its justification which clearly shows that the exponential decay of the M-phase is common to all dimensions.

Integration of Eq. (14) gives the number density of domain of M-phase $N(t) = te^{-v_0 t^2}$. This expression reveals that during the very early stages $N(t)$ rises linearly due to the nucleation of the S-phase, whereas at the late stages $N(t)$ decreases exponentially, which reflects a fast coalescence of the neighboring stable phases as seen in Fig. (1b) [24]. By taking the ratio $\Phi(t)/N(t)$ we confirm that the mean domain size $s(t)$ of the M-phase decays as $s(t) = t^{-1}$. To verify these results we have done Monte Carlo simulation based on the following elaborate algorithm. One time unit of the process in one dimension can be defined as follows:

- (i) At the j th step say there are n number of domains of M-phase of size x_1, x_2, \dots, x_n .
- (ii) Generate a random number R with a uniform distribution within the unit interval $[0, 1]$.
 - (a) Check which of the domains of M-phase contain R . Say, it is the k th domain whose size is x . Then sow a point-like seed exactly at xR and go to step (iii).
 - (b) If R falls within S-phase then increase the iteration step by one unit, and go back to step (ii).

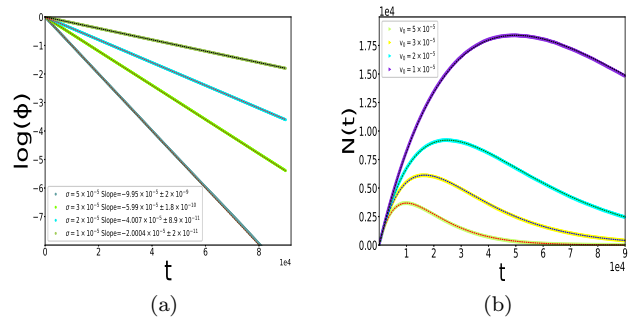


FIG. 2: (a) Plots of $\log(\phi(t))$ versus t of model B are drawn for different σ value that determine the extent of growth velocities v since $v = \sigma/t$. We find straight lines with slope always equal to -2σ which is in complete agreement with our analytical solution given by Eq. (17). (b) The number of domains $N(t)$ of M-phase versus t are shown for model B as a function of time for different constant growth velocities.

- (iii) Increase the size of the seed of S-phase on either side by the constant value v_0 independently. If the domain size of M-phase in any side is less than v_0 then the growth of the S-phase ceases immediately at the point of contact, while it is continuing elsewhere.
- (iv) Increase all the existing domains of S-phase in the same way as described in step (iii).
- (v) Increase the iteration step and the number of domains of M-phase by one unit.
- (vi) Go to step (ii) and continue the process *ad infinitum*.

In Fig. (1) we show the plots of our various results and find that both analytical solutions of the KJMA-process are in perfect agreement to direct numerical simulations.

IV. MODEL B

We now solve Eq. (11) for the growth velocity $v(t) = \sigma/t$ to give

$$c(x, t) = t^2 \exp[-(x + 2\sigma)t]. \quad (16)$$

In this case too, we find that the fraction of the M-phase decays exponentially

$$\Phi(t) = \exp[-2\sigma t], \quad (17)$$

but slower than that for constant velocity. Here the Avrami exponent corresponds to the one that typically known for heterogeneous nucleation and growth processes despite the fact in the present case it strictly describes the homogeneous nucleation [26]. In Fig. (2a) we show plots of $\log(\Phi(t))$ versus t and find a set of straight lines with

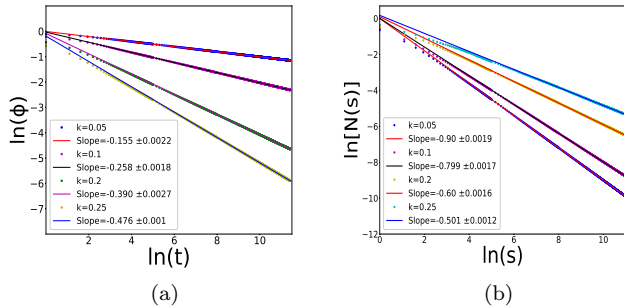


FIG. 3: (a) Plots of $\log(\Phi(t))$ versus $\log(t)$ are drawn for different k values. The result is a set of straight lines with slopes equal to $-2k$ as predicted by our analytical results. In (b) We show plots of $\log(N(s))$ versus $\log(s)$ are shown for different k values and find straight lines with slopes $-(1-2k)$ as predicted by Eq. (25).

slope always equal to 2σ which are in perfect agreement with Eq. (17). This proves that the Avrami exponent not only depends on the nature of the nucleation process but also on the exact choice of the growth velocity. In a similar way we find that the number density of the M-phase varies as

$$N(t) = te^{-2\sigma t}. \quad (18)$$

This reveals that at the early stage $N(t)$ rises linearly like the model (A). However, at the late stage, coalescence events take place less frequently than in the model (A) as shown in Fig. (2b). On the other hand, $N(t)/t$ varies following the same relation with time as $\Phi(t)$ given by Eq. (17). Also for model (B) analytical and numerical results show perfect agreement.

To verify these results we have done Monte Carlo simulation based on the algorithm described in Model A except step (iii) which is replaced as follows.

- Increase the size of the seed of S-phase on either side by σ/j independently provided domain of S-phase is greater than σ in both sides. However, if the domain size of S-phase in any side is less than σ/j then the growth ceases immediately at the point of contact, while it continues elsewhere.

Plots in Fig. (2) are drawn using numerical data based on the above algorithm. We find that our analytical solutions and numerical simulations are in perfect agreement.

V. MODEL C

Next we solve the rate equations for the case $v(x, t) = ks(t)/t$, where k is a dimensionless parameter. Here, we make use of the fact that the mean domain size of the M-phase decays as $s(t) = 1/t$ which is confirmed by numerical simulations and found that such a behaviour is

independent of precise choice of the growth velocity. Incorporating this time dependence into the definition (C) gives $v(x, t) = k/t^2$. Solving Eq. (11) for this front velocity yields

$$c(x, t) = t^{2(1-k)} \exp[-xt]. \quad (19)$$

Unlike the previous two cases, this model is of particular interest for the following reasons. First, all the moments, $M_n(t)$ of $c(x, t)$ where

$$M_n(t) = \int_0^\infty x^n c(x, t) dx, \quad (20)$$

exhibit a power-law

$$M_n(t) \sim t^{-(n-(1-2k))}. \quad (21)$$

Using this relation we find that the mean domain size $s(t)$ of the M-phase decays as

$$s(t) = \frac{M_1(t)}{M_0(t)} = t^{-1}. \quad (22)$$

We find that the mean domain size decays following exactly the same way as for Model (A) and (B). Secondly, unlike the previous two cases, the fraction of the M-phase decays following a power-law

$$\Phi(t) = t^{-2k}. \quad (23)$$

To verify this we plot $\log(\Phi(t))$ versus $\log(t)$ for different k values in Fig. (3a) using simulation data and we find straight lines with slopes equal to $2k$ in each case. It suggests that our numerical results match perfectly with our analytical solution given by Eq. (23).

The physical constraints of the model restrict the feasible range of k values according to Eq. (21). For instance, the lower bound is fixed by the behaviour of $\Phi(t)$ that must be an increasing function of time and hence it demands $k > 0$. On the other hand, the upper bound is fixed by the constraint that the zeroth moment or the number density should be an increasing function of time or at least during the early and/or at intermediate stage. This immediately provides the upper bound $k < 0.5$ since according to Eq. (21) we find

$$M_0(t) = N(t) \sim t^{1-2k} \quad (24)$$

Thus, the only non-trivial and physically interesting k value are the ones that stay within the interval $[0, 0.5]$. One significant result of the present model is that unlike the previous two models here the number density of domains of M-phase keeps increasing at all time (in the scaling regime). This is due to fact that the front velocity is a decreasing function of time resulting in a decelerated motion of the front and hence if the size of the M-phase is large enough the front will effectively stop at some stage leaving a finite sized interface. In passing, we note that in this model again the average domain size $s(t)$ of

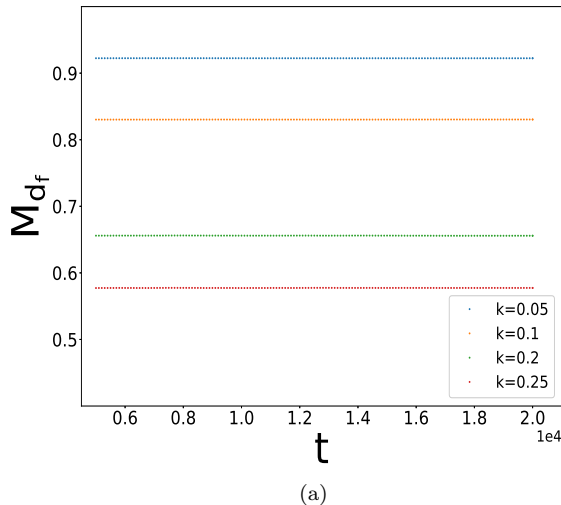


FIG. 4: Plots of the d_f th moment of $c(x,t)$ versus time t are shown for different values of $k < 0.5$. It clearly demonstrates that the d_f th moment is always a conserved quantity suggesting that numerical and analytical results are in perfect agreement.

M-phase decays as $s(t) = t^{-1}$. The existence of scaling and the non-trivial conservation law provides an extra motivation to go beyond the simple scaling description. This can be done by invoking the idea of fractal analysis, as it has been a very useful tool to obtain a global exponent called fractal dimension. To do so, we need a proper yard-stick to measure the size of the set created in the long time limit. The most convenient one is the mean domain size $s(t)$. Using the relation for $s(t)$ we can eliminate t from Eq. (24) and find that the number $N(s)$ scales with yard-stick size or average domain size s following a power-law

$$N(s) \sim s^{-d_f}, \quad (25)$$

where $d_f = (1 - 2k)$ provided $k < 0.5$. The exponent d_f is known as the fractal dimension or the Hausdorff-Besicovitch dimension of the resulting set created by the nucleation and growth process [27–33]. In Fig. (3b) we plot $\log(N(s))$ versus $\log(s)$ using numerical simulation data for different k and find straight line with slope as it should be according to Eq. (25). Once again it proves that numerical simulation and analytical results match perfectly.

Despite the numerical values of the major variables of the system, interval sizes x_i , are changing with time yet according to Eq. (21) we observe that $(1 - 2k)$ th moment of $c(x,t)$ is a conserved quantity. That is, at any given time if there are m number of intervals of M-phase of size x_1, x_2, \dots, x_m then

$$M_{1-2k}(t) = x_1^{1-2k} + x_2^{1-2k} + \dots + x_m^{1-2k} = \text{const.}, \quad (26)$$

regardless of the time and the value of m provided $k < 0.5$

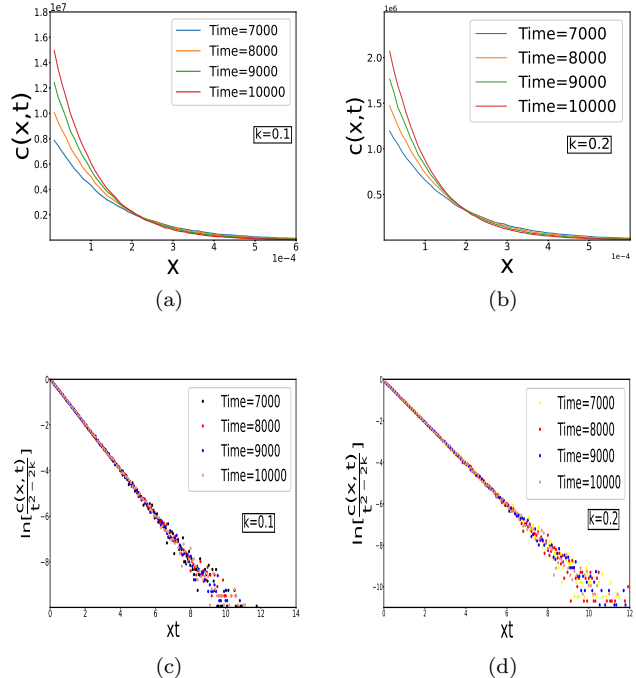


FIG. 5: The plots of the distribution function $c(x,t)$ vs x are shown in (a) and (b) for $k = 0.1$ and $k = 0.2$ respectively. Each plot represents four different times where each set of data represents ensemble average over 1000 independent realizations. In (c) and (d) we plot $\log[c(x,t)/t^{2-2k}]$ vs xt using the data of (a) and (b) respectively and find that all the data collapse into a straight line with slope equal to -1 as suggested by Eq. (19).

(see Fig. (4)). Note that self-similarity along the continuous time axis is a kind of symmetry. Thus, on one hand, we find that the system enjoys dynamical scaling symmetry that manifests itself through data collapse and on the other, we have the $(1 - 2k)$ th moment of the interval size of the M-phase is a conserved quantity in time. The emergence of non-trivial conserved quantity accompanied by continuous self-similar symmetry in time is reminiscent of Noether's theorem as it states that for every symmetry there is a corresponding conservation law and vice versa [34, 35].

We know that if a function $f(x,t)$ of a time varying phenomena satisfies the condition

$$f(x,t) \sim t^\theta \phi(x/t^z), \quad (27)$$

then it is said to obey dynamic scaling [36–38]. The solution for $c(x,t)$ given by Eq. (19) has exactly the same form as in Eq. (27) provided we choose $\theta = 2(1 - k)$ and $z = -1$. Here, the exponent θ and z are fixed by the dimensional requirement that $[f] = [t^\theta]$ and $[x] = [t^z]$ respectively. Thus, the model (c) exhibits dynamic scaling with $\theta = 2(1 - k)$ and $z = -1$. It implies that the numerical value of $c(x,t)$ varies with x for a given time t . That is, the data of $c(x,t)$ versus x will be distinct for

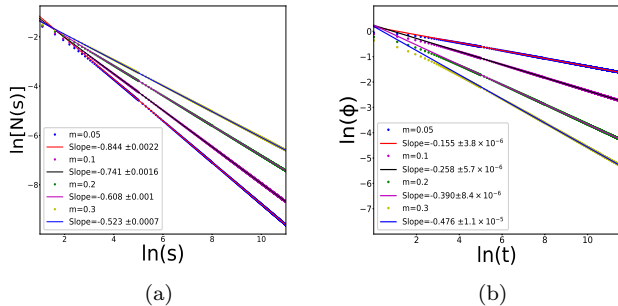


FIG. 6: Plots of $\log(N(s))$ versus $\log(s)$, where N is number of domains of M-phase, are shown in (a) for different m values. In (b) we show plots of $\log(\Phi(t))$ versus $\log(t)$ for different m values. In each case it results in a straight line with slopes always equal to $-d_f$ in (a) and $-(1-d_f)$ in (b). These results match perfectly with our analytical results.

fixed time and for each different k value which can be seen in Figs. (5a) and (5b). However, if we plot $c(x, t)t^{-2(1-k)}$ or $c(x, t)t^{-(1+d_f)}$ versus xt they should collapse into one universal scaling curve. Indeed, they do so, however to show that the scaling function $\phi(\xi)$ is exponential we plot them in the log-linear scaling and find that all the distinct curves in Figs. (5a) and (5b) collapse superbly onto their respective universal curves which are shown respectively in Figs. (5c) and (5d). It means that the solution for the scaling function is exponential. Besides, the data collapse means that the system evolves with time and that the snapshots taken at different times are similar. Since the same system at different times are similar the solutions are self-similar. Self-similarity in this problem manifests, only statistically, through dynamical scaling. This is one of the key properties of fractal too.

To verify these results we have done Monte Carlo simulation based on the algorithm described in Model A except step (iii) which is replaced as follows.

- Increase the size of the seed of S-phase on either side by k/j^2 independently provided domain of S-phase is greater than σ in both sides. However, if the domain size of S-phase in any side is less than σ/j^2 then the growth ceases immediately at the point of contact, while it continues elsewhere.

The data for all the plots shown for this model are obtained by Monte Carlo simulation based on the algorithm described above. The perfect matching with our analytical solution suggests that the algorithm is ideal for describing the integro-differential equation given by Eq. (5) with growth velocity $v = k/t^2$.

VI. MODEL D

Finally, we consider the case where $v(x, t) = mx/\tau$ which implies that the S-phase travels a distance x of

the M-phase in time τ transforming x into the S-phase [23, 38]. However, according to Eq.(5), the typical time between two nucleation events on an interval of size x is $\tau = x^{-1}$ and therefore $v(x, t) = mx^2$ revealing that the growth velocity decreases increasingly fast as the domain size of the M-phase decreases since x itself is a decreasing quantity with time. To solve the model we incorporate the definition of $M_n(t)$ into Eq. (5) and then, after some simple algebraic manipulations, we are able to write the following rate equation for $M_n(t)$

$$\frac{dM_n(t)}{dt} = - \left[\frac{n^2 + n(1 + \frac{1}{2m}) - \frac{1}{2m}}{(n+1)} \right] M_{n+1}(t). \quad (28)$$

Note that for $m = 0$ the total mass or $M_1(t)$ is a conserved quantity. However, for $m > 0$ the system violates this conservation of mass principle due to continuous growth of S-phase at the expense of M-phase. The interesting feature of the above equation is that for each value of m there exists a unique conserved quantity. We can find the value $n = \gamma$ for which the moment $M_\gamma(t)$ is a conserved quantity and it is done simply by setting $dM_n(t)/dt = 0$ [39]. Note that $dM_n(t)/dt = 0$ can be equal to zero either due to $M_{n+1}(t) = 0$ of Eq. (28) or due to its co-factor equal to zero. If the former is zero then it leads to trivial result. On the other hand, if the latter is true then the problem rests on solving a quadratic equation in γ whose real positive root is

$$\gamma(m) = -\frac{1}{2} \left(1 + \frac{1}{2m} \right) + \frac{1}{2} \sqrt{\left(1 + \frac{1}{2m} \right)^2 + \frac{2}{m}}. \quad (29)$$

It implies that the corresponding moment $M_{\gamma(m)}(t)$ is independent of time. It has been verified by numerical simulation as shown in Fig. (7). To find the significance of the value of γ we once again invoke the idea of fractal. Like in model (C), we can use $s(t)$ as a yard-stick and obtain the $N(s)$ we need to cover the system.

We can solve Eq. (28) by assuming a trial solution

$$M_n(t) \sim t^{\alpha(n)}, \quad (30)$$

such that $\alpha(\gamma) = 0$ since $M_\gamma(t)$ is a conserved quantity. Substituting it in Eq. (28) and demanding dimensional consistency we find a recurrence relation

$$\alpha(n+1) = \alpha(n) - 1. \quad (31)$$

Iterating it over and over again subject to the condition that $\alpha(\gamma) = 0$ as required by the conservation law we find that

$$M_n(t) \sim t^{-(n-\gamma(m))}. \quad (32)$$

Using this we find that the average domains of the M-phase $s(t) = M_1(t)/M_0(t)$ decays exactly like all previous three cases i.e., $s(t) = t^{-1}$. We then find that $N(s)$ scales as

$$N(s) \sim s^{-d_f}, \quad (33)$$

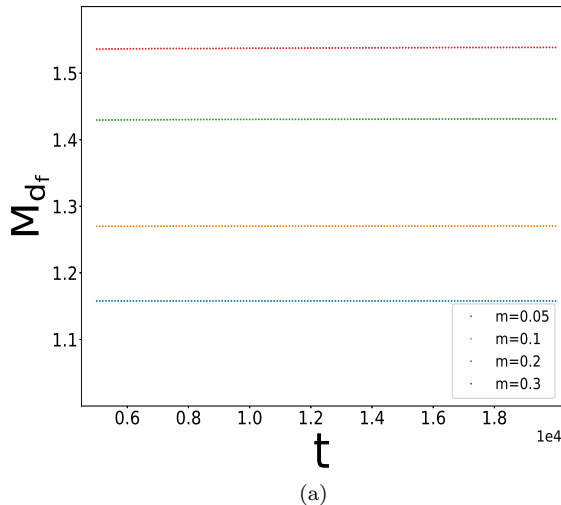


FIG. 7: Here we show that the d_f th moment of $c(x, t)$ is always a conserved quantity for all m values of model D.

where $d_f(m)$ is given by Eq. (29). The plots of $\log(N(s))$ versus $\log(s)$ for different m are shown in Fig. (6a) using data from extensive Monte Carlo simulation and find excellent straight lines with slopes equal to d_f [27, 28]. The exponent d_f is known as the fractal dimension or the Hausdorff-Besicovitch dimension of the resulting set created by the nucleation and growth process [29]. Besides, like in model (C), the Kolmogorov-Avrami formula in this case is no longer valid. Instead, it is replaced by the following general power-law decay of the M-phase

$$\Phi(t) \sim t^{-(1-d_f)}. \quad (34)$$

In Fig. (6b) we show that plots of $\log(\Phi(t))$ versus $\log(t)$ for different m and find that they all obey Eq. (34). This reveals a generalised exponent $(1 - d_f)$ that can quantify the extent of the decay of the M-phase. On the other hand, the coverage by the S-phase $\theta(t)$ reaches its asymptotic value $\theta(\infty) = 1$ as

$$\theta(\infty) - \theta(t) \sim t^{-(1-d_f)}, \quad (35)$$

which is reminiscent of the Feder's law in RSA processes [29].

Finally, we show that the solution for $C(x, t)$ exhibits dynamic scaling. To do this, we check if the solution for $c(x, t)$ obeys dynamic scaling

$$c(x, t) \sim t^{(1+d_f)}\phi(xt). \quad (36)$$

To verify this we plot $c(x, t)$ versus x in Figs. (8a) and (8b) for different m value. According to Eq. (36) the same data would collapse if we divide $c(x, t)$ by t^{V^2} and x by t^{-1} . Indeed, we find excellent data collapse as shown in Figs. (8c) and (8d) respectively for $m = 0.05$ and $m = 0.1$. It provides a clear litmus test of our solution

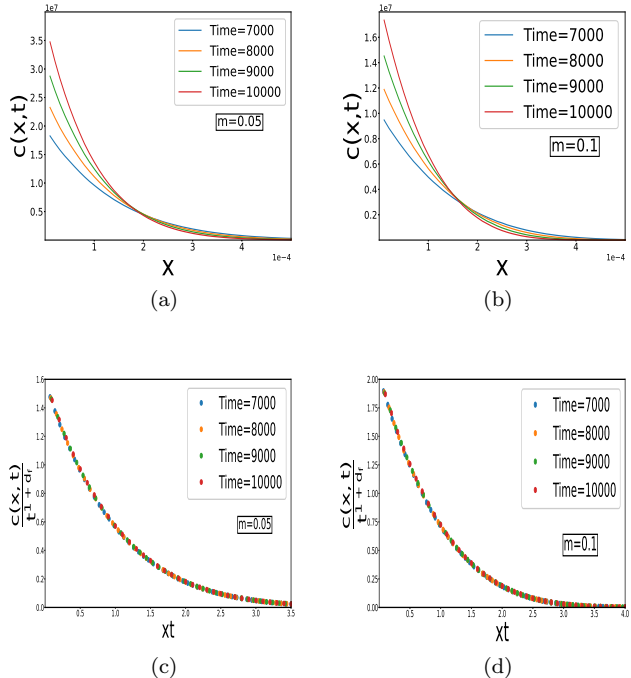


FIG. 8: Plots of $c(x, t)$ versus x for (a) $m = 0.05$ and (b) $m = 0.1$ are drawn as a representative values of m . In (c) and (d) we plot $c(x, t)t^{-(1+d_f)}$ versus xt and we find excellent data collapse of the same data of (a) and (b) respectively which confirms that the model D obeys dynamic scaling.

that it obeys dynamic scaling and hence like model C, the snapshots of the model D too taken at different times are similar. It is worth to mention that the number density in (C) and (D) increases for all time - a sharp contrast to the models (A) and (B) where $N(t)$ increases only at the early stage. This is due to the fact that in models (C) and (D), the growth velocity decreases in time in such a way that two growing phases from opposite direction hardly coalesce. In fact, the growth of the S-phase virtually stops at some stage.

To verify these results we have done Monte Carlo simulation based on the algorithm described in Model A except step (iii) which is replaced as follows.

- Increase the size of the seed of S-phase on each side by an amount equal to square of the respective domain size of the M-phase and the growth ceases immediately at the point of contact, while it continues elsewhere.

VII. DISCUSSION OF FINDINGS AND SUMMARY

In this article, we have studied a class of random nucleation and growth processes of a stable phase with three different growth velocities which can be space and time

Model	$\Phi(t)$	$N(t)$	$s(t)$	Scaling	Fractal
$v = v_0$	$e^{-v_0 t^2}$	$t e^{-v_0 t^2}$	t^{-1}	violates	\times
$v = \sigma/t$	$e^{-2\sigma t}$	$t e^{-2\sigma t}$	t^{-1}	violates	\times
$v = ks(t)/t$	$t^{-(1-d_f)}$	t^{d_f}	t^{-1}	obeys	$(1-2k)$
$v = mx^2$	$t^{-(1-d_f)}$	t^{d_f}	t^{-1}	obeys	$d_f(m)$

TABLE I: Summary of the various model results

dependent. Also, we revisit the classical KJMA model. The three new growth velocities describe a process in which the growth velocity depends on the local configuration of the system at every instant of time. We have solved the models analytically and verified the results by extensive Monte Carlo simulation. One interesting finding is that in all four cases the mean domain size $s(t)$ of M-phase decays following a power-law $s(t) \sim t^{-\alpha}$ with the same exponent $\alpha = 1$ irrespective of the detailed choice of the growth velocity. There must be a common mechanism behind this common nature. Indeed, all the four models share one common thing, i.e. the nucleation process is described by the random secession model. However, the fraction of the untransformed space (M-phase) and the corresponding number density are very sensitive to the specific choice of the growth velocity.

The most striking result, though, is the emergence of fractal for either fully time dependent or fully size dependent growth velocities in the sense that the growth velocities are either proportional to inverse square of time t or simply proportional to the square of size x . The system is called fractal if the exponent of the power-law decay of $N(s)$ as a function of s is less than the dimension $d = 1$ of the space where the system is embedded and at the same time the system must be self-similar. One of the ways to test whether the systems that evolves probabilistically with time is self-similar or not is that it must exhibit dynamic scaling. Testing of dynamic scaling means that the numerical values of the dimensional quantities such as $c(x, t)$ and x at different time will be different but the corresponding dimensionless quantities $c(x, t)/t^{\theta z}$ and x/t^z would coincide. In other words, the plots of $c(x, t)$ versus x for time will be distinct but all these distinct plots would collapse if we plot $c(x, t)/t^{\theta z}$ versus x/t^z instead. We find $\theta = 1 + d_f$ and $z = -1$ for both model C and D albeit the fractal dimension d_f is different. The self-similarity is also a kind of continuous

symmetry along the continuous time axis. Interestingly, we also find that during the evolution the d_f th moment is always a conserved quantity. These two results are reminiscent of Noether's theorem that states that for every continuous symmetry there must exist a conserved quantity. We have also shown that when either the temporal variable t or both spatial and the temporal in the definition of the velocity are assumed constant, the decay of the metastable phase is always exponential and is also accompanied by the violation of scaling. One of the key observables in nucleation and growth processes is how the fraction of the M-phase decays to let the new S-phase grow. We find that both in model C and D, it decays following a power-law with a unique generalised exponent $(1 - d_f)$ though the d_f values are different.

Thus, the present work represents the most obvious natural extension of the classical KJMA theory. We believe that this extension is a realistic description for many natural processes. Furthermore, our model sketches the process of invasion and growth of a biological colony with a random immigration of pioneer individuals or seed arrival. One important example is the spread of diseases such as fungal spots on plant leaves. Here one assumes that spores are transmitted by wind or insects and randomly arrive on the leave surface. Once an infected spot is established it stays and begins to grow. In many studies of such biological processes the growth has been found to deviate from the constant velocity assumption of the KJMA model. Instead it is typically observed that the velocity increases with the increase in proportion of non-infected areas, i.e. the M-phase (Vanderplank principle [40]). Therefore we believe that the present investigation of the consequences of state-dependent growth velocities will have important applications.

We conclude with the following words. The power-law decay of the M-phase can be assumed to be a generalized formula replacing the classical Kolmogorov-Avrami law, provided, the distribution of the M-phase in the late stage describes a scale-free fractal. The fractal dimension is the quantitative measure of the notion that the density of the M-phase is less at larger length scale. We believe that the present work will have a significant impact in changing the way we intended to interpret the experimental data as we are now aware of the fascinating results due to the decelerating growth velocity.

[1] J. W Christian, *The Theory of Phase Transformations in Metals and Alloys*, (Pergamon Press, New York, 1981).
[2] A. J. Bray, *Adv. Phys.* **43** 357 (1994).
[3] D. Kong, Z. Zheng, F. Meng, N. Li, D. Li, *J. of the Electrochem. Soc.* 165 (2018).
[4] R. L. Jack and L. Berthier, *J. Chem. Phys.* **144** 244506 (2016).
[5] Y. Pomeau and M. Ben Amar in *Solids Far From Equilibrium*, edited by C. Godr che (Cambridge University

Press, Cambridge, 1992).
[6] Y. Yamada, N. Hamaya, J. D. Axe, and M. Shapiro, *Phys. Rev. Lett.* **53**, 1665 (1984); H. Hermann, N. Matern, S. Roth, and P. Uebele, *Phys. Rev. B* **56**, 13888 (1997).
[7] K. Matyjasek, *J. Phys. D: Appl. Phys.* **34**, 2211 (2001); Y. Ishibashi and Y. Takagi, *J. Phys. Soc. Jpn.* **31**, 506 (1971).
[8] M. Arim, S. R. Abades, P. E. Neill, M. Lima, and P. A.

- Marquet, PNAS **103** 374 (2005).
- [9] P. Meakin, Rep. Prog. Phys. **55** 157 (1992).
- [10] G. Giacomelli, F. Marino, M. A. Zaks and S. Yanchuk, Phys. Rev. E **88** 062920 (2013).
- [11] A. N. Kolmogorov, Bull. Acad. Sci. USSR, Phys. Ser. **1**, 355 (1937); M. Avrami, J. Chem. Phys. **7**, 212 (1940) ; M. Avrami, *ibid.* **9**, 177 (1941); W. A. Johnson and P. A Mehl, Trans. AIMME **135**, 416 (1939).
- [12] K. Sekimoto, *Phys. Lett. A* **105**, 390 (1984); Ken Sekimoto, Physica A **135A**, 328 (1986).
- [13] K. Sekimoto, *Physica 125A* 261 (1984); K. Sekimoto, *Physica 128A* 132 (1984);
- [14] D. Crespo and T. Pradell, Phys. Rev. B **54**, 3101 (1996).
- [15] R. M. Bradley and P. N. Strenski, Phys. Rev. B **40**, 8967 (1989).
- [16] C. W. Price, Acta Metal. Mater. **38**, 727 (1990).
- [17] M. Castro, F. Dominguez-Adame, A. Sanchez, and T. Rodriguez, Appl. Phys. Letters, **75**, 2205 (1999); M. Fanfoni and M. Tomellini, Phys. Rev. B **54**, 9828 (1996); V. Erukhimovitch and J. Baram, *ibid.* **50**, 5854 (1994).
- [18] H. Su, Y. Wang, L. Ren, P. Yuan, B. K. Teo, S. Lin, L. Zheng, and N. Zheng, Inorg. Chem. **58** 259 (2019).
- [19] M. R. Riedel, S. Karato, Geophys. J. Int. **125** 397 (1996).
- [20] S. Labidi, Z. Jia, M. B. Amar, K. Chhora and A. Kanaev, Phys. Chem. Chem. Phys. **17** 2651 (2015).
- [21] S. Tieng, O. Brinza, K. Chhor and A Kanaev, J Sol-Gel Sci Technol **64** 145 (2012).
- [22] M. R. Riedel and S. Karato, Geophys. J. Int. **125**,397 (1996).
- [23] D. L. Maslov, Phys. Rev. Lett. **71**, 1268 (1993).
- [24] E. Ben-Naim and P. L. Krapivsky, Phys. Rev. E **54**, 3562 (1996).
- [25] R. M. Ziff and E. D. McGrady, J. Phys. A **18**, 3027 (1985).
- [26] E. D. Zanotto and M. C. Weinberg, J. Non-Crys. Solids **105**, 53 (1988).
- [27] M. K. Hassan, M. Z. Hassan, Phys. Rev. E **79** 021406 (2009).
- [28] M. K. Hassan, M. Z. Hassan and N. Islam, Phys. Rev. E **88** 042137 (2013).
- [29] J. Feder, *Fractals*, (Plenum, New York, 1988).
- [30] S. Banerjee, M. K. Hassan, S. Mukherjee and A Gowrisankar, *Fractal Patterns in Nonlinear Dynamics and Applications* (CRS press, Taylor & Francis group, New York, 2020).
- [31] M. K. Hassan and J. Kurths, Phys. Rev. E **64** 016119 (2001).
- [32] M. K. Hassan and G. J. Rodgers, Phys. Lett. A **208** 95 (1995).
- [33] M. K. Hassan and J. Kurths, Physica A **315** 342 (2002).
- [34] M K Hassan, Eur. Phys. J Spec. Top. **228** 209 (2019).
- [35] R. Rahman, F. Nowrin, M. S. Rahman, J. A. Wattis, M. K. Hassan, Phys. Rev. E **103** 022106 (2021).
- [36] M. K. Hassan, M Z. Hassan and N. I Pavel, J. Phys. A: Math. Gen. **44** 175101 (2011).
- [37] D. Sarker, L. Islam, M. K. Hassan, Chaos, Solitons & Fractals, **132** 109591 (2020).
- [38] M. K. Hassan and M. Z. Hassan, Phys. Rev. E **77** 061404 (2008).
- [39] P. L. Krapivsky and E. Ben-Naim, Phys. Lett. A **196** 168 (1994).
- [40] J. Vanderplank, Plant Diseases: Epidemics and Control (Acad. Press, NY, 1963).